JACS
JOURNAL OF THE AMERICAN CHEMICAL SOCIETY
Article
pubs.acs.org/JACS

AMHB: (Anti)aromaticity-Modulated Hydrogen Bonding

Tayeb Kakeshpour,[†] Judy I. Wu,*[,‡] and James E. Jackson*[,†]

[†]Department of Chemistry, Michigan State University, East Lansing, Michigan 48824, United States
[‡]Department of Chemistry, University of Houston, Houston, Texas 77204, United States

Supporting Information

ABSTRACT: This *in silico* survey shows that changes in the (anti)aromatic character of π-conjugated heterocycles can be used to fine-tune their hydrogen (H-)bond strengths. Upon H-bonding dimerization, the π-electrons of these rings can be polarized to reinforce or disrupt their (anti)aromatic π-conjugated circuits (πCCs) and stabilize or destabilize the resulting H-bonded complexes. H-bonding interactions that enhance aromaticity or relieve antiaromaticity are fortified, whereas those that intensify antiaromaticity or disrupt aromaticity are weakened, relative to analogues lacking full π-circuits. Computed dissected nucleus-independent chemical shifts, NICS(1)$_{zz}$, reveal a uniform pattern and document changes in the magnetic (anti)aromatic character of the heterocycles considered. Recognition of this (anti)aromaticity-modulated H-bonding (AMHB) phenomenon offers insights into a range of fields from organocatalysis and self-assembly to pharmaceutical chemistry and molecular biology.

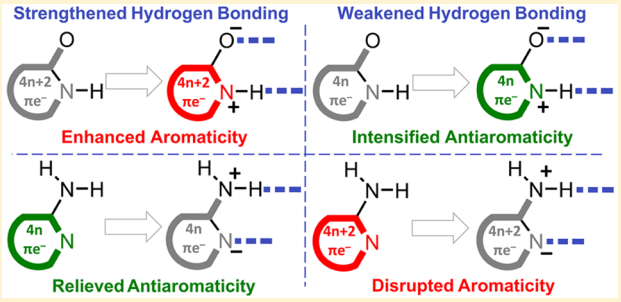

INTRODUCTION

This paper introduces the general phenomenon of (anti)-aromaticity-modulated hydrogen (H-)bonding (AMHB). By polarizing the π-systems of heterocyclic rings with π-conjugated circuits (πCCs), H-bonding interactions may perturb their cyclic $4n$ or $(4n + 2)$ π-electron (πe^-) delocalization to enhance or reduce their (anti)aromatic character. As a result, H-bonded complexes of heterocycles with the same donor and acceptor moieties can exhibit drastically different association energies, depending on their ring π-conjugation patterns (see Figure 1a,c,d,f). Like many other structure-H-bonding relationships, (e.g., resonance-assisted H-bonding,[1] H-bond cooperativity,[2] and strain-induced H-bonding[5]), the AMHB pattern suggests ways to fine-tune the energetics of H-bonded systems.[3]

Figure 1 displays examples representing the four cases of AMHB. As a consequence of AMHB, the H-bonding dimerization enthalpy of 2-pyridone (Figure 1a, increased aromaticity upon H-bonding) is stronger than for both formamide (Figure 1b, no AMHB) and its four-membered ring azet-2(1H)-one analog (Figure 1c, increased antiaromaticity upon H-bonding). Conversely, in the 2-aminopyridine case (Figure 1d), dimerization disrupts aromaticity in the six-membered ring, resulting in a lower dimerization energy compared to that of formamidine (Figure 1e) and the analogous four-membered ring azet-2-amine (Figure 1f, relieved antiaromaticity upon H-bonding). Changes in bond lengths upon dimerization (shown in dashed boxes in Figure 1) point to electron polarization effects that enhance the resonance forms shown in the dimer structures.

Despite aromaticity and H-bonding being known as separate concepts for decades, their reciprocal connection and its effects on H-bond strengths received little notice until recently.[6,7] Dewar first proposed that intramolecular H-bonding can enhance 6 πe^- delocalization, increasing the aromatic character of nonbenzenoid rings like tropolone and its derivatives.[8,9] Maksic et al. proposed that ring π-aromatization increased the proton affinities of organic superbases.[10−12] More recently, aromatic gain was invoked on the basis of nucleus-independent chemical shifts (NICS) computations to explain the superior H-bond-donating ability of squaramide over urea-based organocatalysts[13,14] and to design self-assembling squaramide-based polymers.[15] However, related computational studies questioned this analysis.[16] By searching for the broader pattern of both positive and negative AMHB effects across a diversity of heterocycles, the present work obviates such framework-specific controversies.

This study focuses on examples of the AMHB effect in heterocyclic five-membered rings to avoid (a) the complications of ring strain in three- and four-membered rings; (b) the arbitrariness of choosing breached πCC reference compounds for six-membered or larger rings; and (c) the conformational complexity of larger cycles. Many biologically and pharmaceutically significant species include five-membered heterocyclic moieties akin to those examined herein.[17−24] Thus, beyond its conceptual interest, an appreciation of AMHB may help guide studies of biomedical significance.

COMPUTATIONAL DETAILS

All gas-phase geometries for monomers and dimers in Figures 2, 3, and 5−7 were fully optimized employing Gaussian09[25] at

Received: December 4, 2015
Published: February 10, 2016

DOI: 10.1021/jacs.5b12703
J. Am. Chem. Soc. 2016, 138, 3427−3432

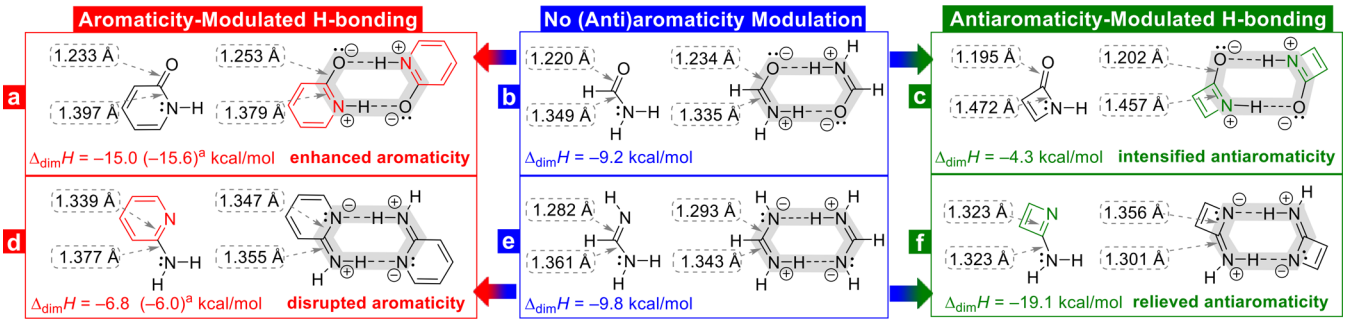

Figure 1. Examples of H-bonded dimers with and without AMHB. All dimerization enthalpies and bond distances were computed at PBE0/6-311++G(3df,3dp)//PBE0/aug-cc-pVDZ in implicit benzene solvent. Experimental values[4,5] (indicated by footnote a) are listed for comparison. Nonbonding electron pairs not involved in π-delocalization are omitted in all figures for visual simplicity.

Scheme 1. Generation of Examples for the Four AMHB Cases

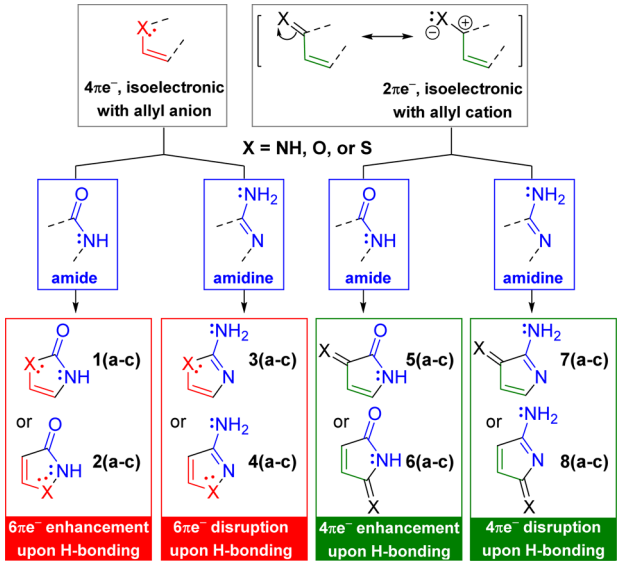

the PBE0/6-311++G(3df,3pd) level.[26−30] At this level, the mean absolute error for the computed interaction energies of the formic acid, formamide, and formamidine dimers has been shown to be only 0.53 kcal/mol when benchmarked against CCSD(T) results extrapolated to the complete basis set (CBS) limit.[31] Frequency calculations verified that all monomer and dimer stationary points have zero imaginary frequencies. Dimerization energies $\Delta_{dim}E$ [= E_{dimer} − 2$E_{monomer}$] were computed at the aforementioned level,[31,32] with no vibrational corrections. E_{dimer} is total electronic energy of the dimer, and $E_{monomer}$ is total electronic energy of the monomer. $\Delta\Delta_{dim}E$ evaluates the $\Delta_{dim}E$ difference between the fully πCCs (e.g., **1(a-c)-8(a-c)**) and their reference species with breached πCCs (e.g., **1′(a-c)-8′(a-c)**).

As they are referenced to experimental data, the dimerization enthalpies ($\Delta_{dim}H$) in Figure 1 were computed at PBE0/6-311++G(3df,3dp)//PBE0/aug-cc-pVDZ[33−35] in implicit benzene solvent, simulated by the conductor-like polarizable continuum model.[36,37]

Dissected nucleus-independent chemical shifts, NICS(1)$_{zz}$, at the PW91/6-311++G(3df,3pd)//PBE0/6-311++G(3df,3pd) level,[38] were computed at points 1 Å above ring centers to quantify changes in (anti)aromatic character of the monomers upon dimerization. NICS(1)$_{zz}$ extracts the out-of-plane (zz) tensor component of the isotropic NICS, thus minimizing σ-orbital contributions.[39] Negative values of ΔNICS(1)$_{zz}$ [= NICS(1)$_{zz(dimer)}$ − NICS(1)$_{zz(monomer)}$] upon H-bonded dimer formation indicate increased diatropic (i.e., aromatic) or decreased paratropic (i.e., antiaromatic) character, and positive ΔNICS(1)$_{zz}$ values signify the opposite.

RESULTS AND DISCUSSION

Depending on their π-conjugation patterns, heterocyclic H-bonded dimers may display H-bond-induced (anti)aromaticity enhancement or weakening effects. To generate examples for these four possible cases, amide and amidine moieties are embedded in π-conjugated cycles (Scheme 1). Via fusion of the amide residue [−CO−NH−] to 4 πe^- fragments (Scheme 1, first column), 6 πe^- πCCs are generated in which aromaticity may be enhanced upon H-bonding (i.e., **1(a-c)$_{dimer}$**, Figure 2). On the other hand, if the amidine moiety [−(NH$_2$)C=N−] is fused to the 4 πe^- fragments (Scheme 1, second column), aromatic 6 πe^- heterocycles are obtained whose aromaticity is disrupted by H-bonding (i.e., **2(a-c)$_{dimer}$**, Figure 3). Complementary cases for studying antiaromaticity effects are created by fusion with 2 πe^- complementary residues. Connecting the amide residue to them (Scheme 1, third column), 4 πe^- πCCs are fashioned whose antiaromaticity may be reinforced by H-bonding (i.e., **3(a-c)$_{dimer}$**, Figure 5). Finally, −C=N− fusion of the amidine to the above 2 πe^- fragments (Scheme 1, fourth column) forms structures whose antiaromaticity is partially relieved upon H-bonding (i.e., **4(a-c)$_{dimer}$**, Figure 6).

Coupling of H-Bonding and Aromaticity. *H-bond Strengthening by Enhancement of Aromaticity.* Figure 2 shows compounds that are expected to display aromaticity enhancement upon H-bonding. Based on their computed NICS(1)$_{zz}$ values, **1(a-c)** (−14.9 to −12.0 ppm) and **2(a-c)** (−14.3 to −11.6 ppm) are modestly aromatic, due to amide π-delocalization. This delocalization is reinforced upon H-bonding in **1(a-c)$_{dimer}$** and **2(a-c)$_{dimer}$**, increasing the 6 πe^- character of the rings and hence their aromaticities (see Figure 2 for resonance forms). More negative NICS(1)$_{zz}$ values confirm the enhanced aromaticities upon H-bonding [**1(a-c)$_{dimer}$**: −16.7 to −13.5 ppm, **2(a-c)$_{dimer}$**: −18.1 to −15.8 ppm] (see Figure 2).

Due to H-bond-induced aromatization, the calculated dimerization energies (see $\Delta_{dim}E$ in the table in Figure 2) for **1(a-c)$_{dimer}$** and **2(a-c)$_{dimer}$** are 2.4 to 5.3 kcal/mol more negative than those of the analogous dimers **1(a-c)′$_{dimer}$-2(a-c)′$_{dimer}$**, in which no AMHB is possible. The 1.1−3.5 kcal/mol larger $\Delta_{dim}E$'s for **2(a-c)** (heteroatoms at 1,2-positions) compared to their **1(a-c)** constitutional isomers may in part

DOI: 10.1021/jacs.5b12703
J. Am. Chem. Soc. 2016, 138, 3427−3432

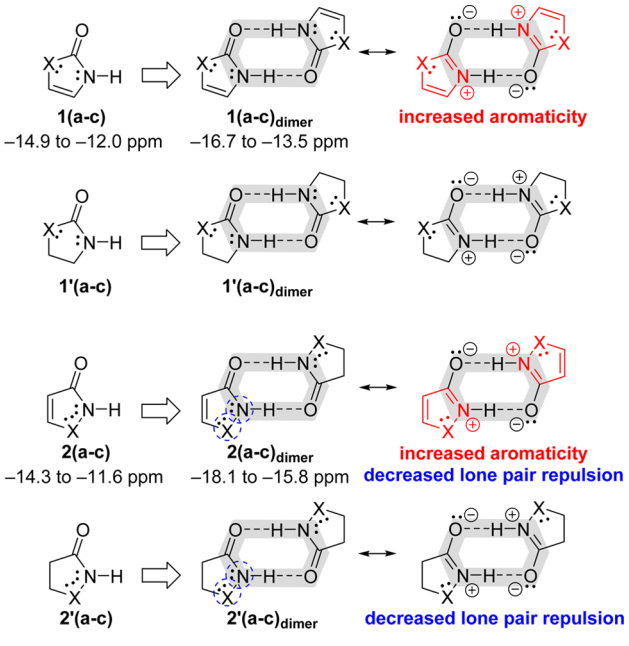

Cpd.	*X*	$\Delta_{dim}E$	*Cpd.*	$\Delta_{dim}E$	$\Delta\Delta_{dim}E$	$\Delta NICS(1)_{zz}$
1a	NH	–19.2	1a'	–14.8	–4.4	–1.8 ppm
1b	O	–18.7	1b'	–15.6	–3.1	–1.4 ppm
1c	S	–17.5	1c'	–14.6	–2.9	–1.5 ppm
2a	NH	–21.0	2a'	–18.6	–2.4	–4.8 ppm
2b	O	–19.8	2b'	–16.9	–2.9	–4.2 ppm
2c	S	–21.0	2c'	–15.7	–5.3	–2.4 ppm

Figure 2. AMHB strengthens H-bonding interactions in the dimers of **1** and **2** in contrast to their breached congeners, **1**′ and **2**′.

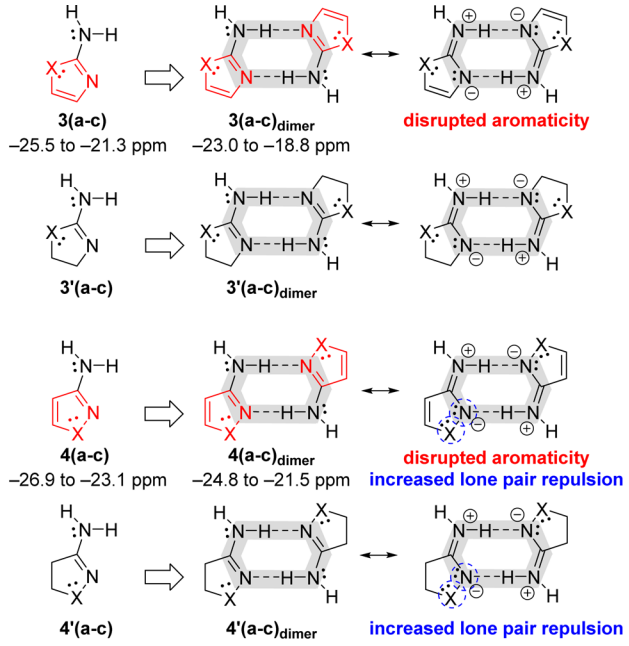

Cpd.	*X*	$\Delta_{dim}E$	*Cpd.*	$\Delta_{dim}E$	$\Delta\Delta_{dim}E$	$\Delta NICS(1)_{zz}$
3a	NH	–13.1	3a'	–14.5	+1.4	+2.5 ppm
3b	O	–14.1	3b'	–14.9	+0.8	+1.3 ppm
3c	S	–12.5	3c'	–14.2	+1.7	+3.0 ppm
4a	NH	–7.9	4a'	–11.6	+3.7	+2.0 ppm
4b	O	–11.1	4b'	–13.2	+2.1	+1.7 ppm
4c	S	–9.8	4c'	–12.6	+2.8	+2.0 ppm

Figure 3. AMHB weakens H-bonding interactions in the dimers of **3** and **4** in contrast to their breached congeners, **3**′ and **4**′.

reflect relief of π-lone pair repulsion between the neighboring N–H and X (X = NH, O, or S) groups in **2(a-c)**$_{dimer}$ (see Figure 2, blue dotted circles) as suggested by the N–X bond length decrease in **2(a-c)** upon dimerization.

H-bond Weakening by Disruption of Aromaticity. H-bonding examples that disrupt 6 πe^- aromaticity are shown in Figure 3. Since both **3(a-c)** and **4(a-c)** are aromatic, they have large negative NICS(1)$_{zz}$ values [**3(a-c)**: –25.5 to –21.3 ppm and **4(a-c)**: –26.9 to –23.1 ppm] (Figure 3), and their H-bonded dimers, **3(a-c)**$_{dimer}$-**4(a-c)**$_{dimer}$, display decreased aromatic character (see Figure 3 for resonance forms) as confirmed by reduced diatropicity [**3(a-c)**$_{dimer}$: –23.0 to –18.8 ppm, **4(a-c)**$_{dimer}$: –24.8 to –21.5 ppm]. Thus, the $\Delta_{dim}E$ values for the partially "de-aromatized" **3(a-c)**$_{dimer}$-**4(a-c)**$_{dimer}$ are 0.8–3.7 kcal/mol weaker than their **3(a-c)**′$_{dimer}$-**4(a-c)**′$_{dimer}$ analogues, which lack H-bond/aromaticity coupling. Increased π-lone pair repulsion between the neighboring N and X (X = NH, O, or S) heteroatoms further weakens the H-bonding interactions of **4(a-c)**$_{dimer}$, as confirmed by the increased N–X bond lengths and the 2.7 to 5.2 kcal/mol weaker $\Delta_{dim}E$'s compared to **3(a-c)**$_{dimer}$ (see Figure 3).

A survey of the online Cambridge Structural Database (WebCSD),[40] in which H-bond-donor/-acceptor distances were compared, found that the average distance for **2a** in five crystals of its derivatives[41−45] is 0.147 Å shorter (2.703(2) vs 2.850(4) Å, see Figure 4a) than for **2a**′ in 12 crystal structures.[46−56] Conversely, the average N···N distance in **3a** derivatives in three crystal structures[57−59] is 0.110 Å longer (3.013(3) vs 2.903(3), see Figure 4b) than **3a**′ derivatives in five crystal structures.[60−63] These observations offer strong

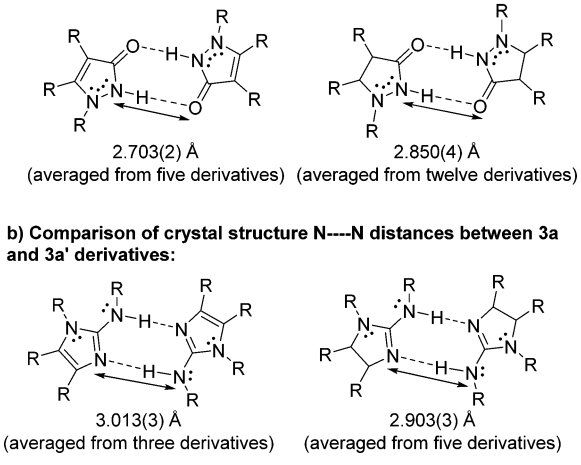

Figure 4. Comparison of X-ray crystal structure H-bond donor-acceptor distances for (a) **2a** vs **2a**′ derivatives and (b) **3a** vs **3a**′ derivatives. R groups may be H, alkyl, phenyl, or various substituted aryl groups, out of the plane of the five-membered rings. These derivatives were found using the substructure search tool available on the WebCSD webpage, followed by a manual refinement to eliminate examples that either did not form H-bonded dimers or had strong electron-withdrawing/-donating groups perturbing their πCCs or H-bond-donor/-acceptors directly.

DOI: 10.1021/jacs.5b12703
J. Am. Chem. Soc. 2016, 138, 3427–3432

experimental support for the notion of aromaticity assisted H-bonding and aromaticity disrupted H-bonding in the cases of **2a** and **3a**, respectively.

Coupling of H-Bonding and Antiaromaticity. Heterocyclic rings with formal 4 πe^- counts, i.e. antiaromatic systems such as **5(a-c)**-**8(a-c)** in Figures 5 and 6, also can exhibit enhanced or reduced H-bond strengths depending on their π-conjugation patterns. H-bonding interactions that intensify cyclic 4 πe^- delocalization are weakened; those that relieve antiaromaticity by disrupting cyclic conjugation are strengthened.

H-bond Weakening by Intensification of Antiaromaticity. Compounds in Figure 5 are expected to increase in antiaromatic character upon dimerization. The positive shifts of their NICS(1)$_{zz}$ values [**5(a-c)**: +3.6 to +7.2 ppm; **6(a-c)**: −4.0 to −1.1 ppm; **5(a-c)$_{dimer}$**: +3.6 to +7.3 ppm; and **6(a-c)$_{dimer}$**: −3.7 to −0.5 ppm] reflect this effect. As a result of opposing H-bond/antiaromaticity effects, the dimerization energies for **5(a-c)** are smaller than those of their **5(a-c)′** reference compounds. In **6(a-c)**, the two electron-withdrawing groups in the 2 and 5 positions of the five-membered rings strongly localize the nitrogen lone pair, isolating it from the endocyclic double bond. This isolation results in less antiaromaticity in **6(a-c)** than in **5(a-c)**, as seen by comparing their NICS(1)$_{zz}$ values (see Figure 5), and hence a smaller effect on **6** than on **5**.

H-bond Strengthening by Disruption of Antiaromaticity. Complementary to the other three cases discussed so far, Figure 6 compiles examples in which antiaromaticity is relieved upon H-bonding. The upfield shift of NICS(1)$_{zz}$ values of monomers **7(a-c)** (+10.4 to +19.3 ppm) when dimerized to **7(a-c)$_{dimer}$** (+8.9 to +12.6 ppm) indicates a decrease in antiaromatic character upon H-bonding. As a result of this relaxation of antiaromatic destabilization, the dimerization energies for **7(a-c)** are 4.2−6.0 kcal/mol more favorable than those of **7(a-c)′** in which no AMHB is possible due to the breached ring πCC. Series **8(a-c)** were expected to show similar coupling, but only **8b** expresses any significant antiaromaticity/H-bonding coupling. The weak effect in **8(a,c)** is likely due to the lower intrinsic antiaromatic character of **8(a,c)** (NICS(1)$_{zz}$: −4.1 to −2.0 ppm) compared to **7(a-c)** (NICS(1)$_{zz}$: +10.4 to +19.3 ppm), presumably due to ring π-electron isolation by the carbonyl and C=X groups in 1- and 3-positions, and hence decreased electron delocalization around the πCC.

Tuning Association Energies via AMHB. 1H-imidazo[1,2-*a*]imidazole (Figure 7) is a framework in which dimerization energy could in principle be tuned from favorable to unfavorable through hydrogenation of different C=C π-bonds. In **9$_{dimer}$**, H-bonding enhances a resonance form in which an aromatic Clar sextet[64] is formed as an imidazolium ring, while an imidazole sextet is disrupted. The expected changes in ring currents are clearly observed by probing ΔNICS(1)$_{zz}$ for both rings. The ΔNICS(1)$_{zz}$ is +2.5 ppm for

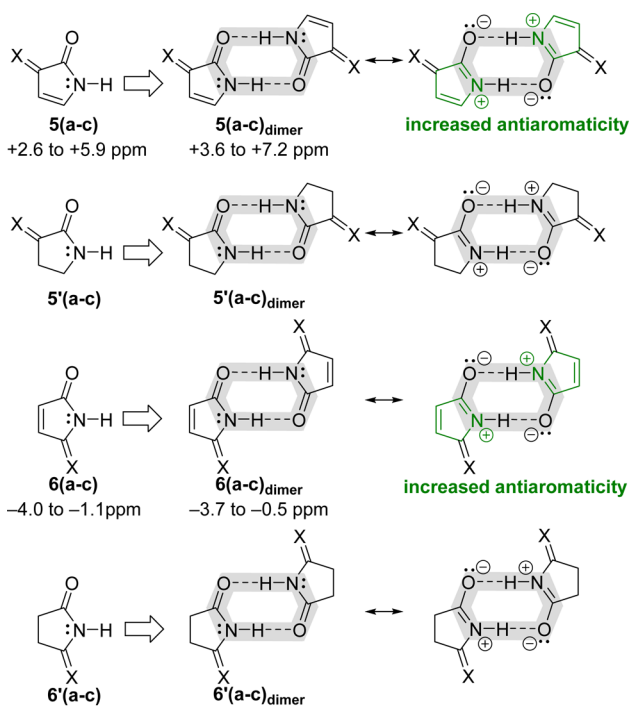

Cpd.	*X*	$\Delta_{dim}E$	*Cpd.*	$\Delta_{dim}E$	$\Delta\Delta_{dim}E$	$\Delta NICS(1)_{zz}$
5a	NH	−14.4	5a'	−15.9	+1.5	+1.0 ppm
5b	O	−15.0	5b'	−17.3	+2.3	+1.3 ppm
5c	S	−15.2	5c'	−17.1	+1.9	+1.9 ppm
6a	NH	−11.2	6a'	−11.3	+0.1	+0.3 ppm
6b	O	−11.1	6b'	−12.1	+1.0	+0.6 ppm
6c	S	−11.0	6c'	−11.1	+0.1	+0.6 ppm

Figure 5. AMHB weakens H-bonding interactions in the dimers of **5** and **6** in contrast to their breached congeners, **5′** and **6′**.

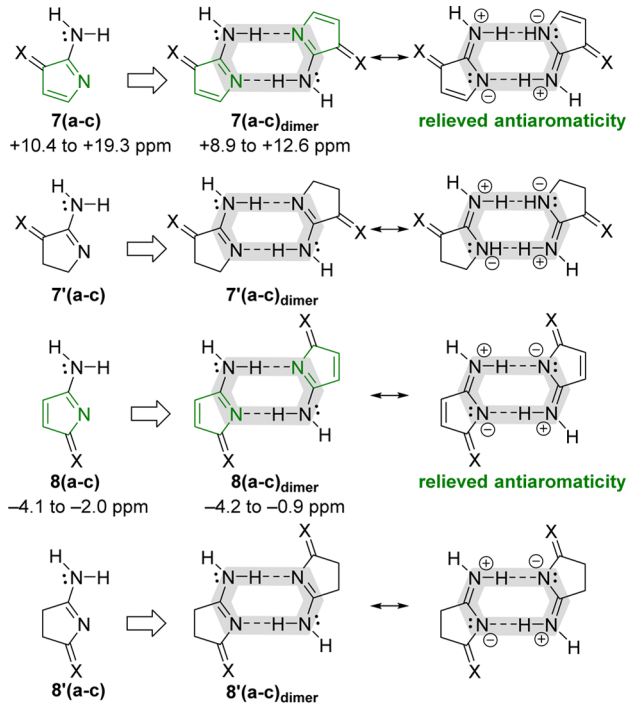

Cpd.	*X*	$\Delta_{dim}E$	*Cpd.*	$\Delta_{dim}E$	$\Delta\Delta_{dim}E$	$\Delta NICS(1)_{zz}$
7a	NH	−16.9	7a'	−12.7	−4.2	−1.5 ppm
7b	O	−17.8	7b'	−13.0	−4.8	−2.5 ppm
7c	S	−18.3	7c'	−12.3	−6.0	−6.6 ppm
8a	NH	−16.8	8a'	−15.8	−1.0	−0.1 ppm
8b	O	−22.9	8b'	−21.1	−1.8	−0.7 ppm
8c	S	−23.7	8c'	−23.3	−0.4	−0.6 ppm

Figure 6. AMHB strengthens H-bonded dimers of **7** and **8** in contrast to breached congeners **7′** and **8′**.

DOI: 10.1021/jacs.5b12703
J. Am. Chem. Soc. 2016, 138, 3427−3432

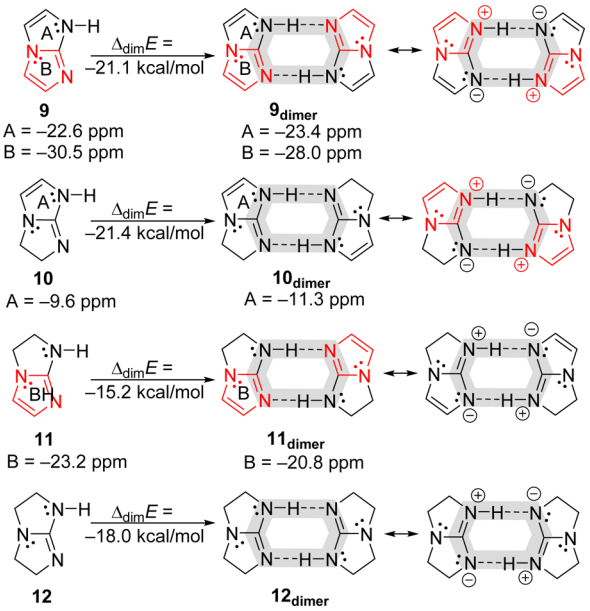

Figure 7. 1H-imidazo[1,2-*a*]imidazole dimer and its hydrogenated analogues. The resonance forms that are enhanced via H-bonding are shown on the right. The aromatic Clar sextet rings are in red.

the imidazole ring, whereas it is −0.8 ppm for the nonsextet ring (Figure 7).

Comparison of dimerization energies between $\mathbf{9}_{\mathbf{dimer}}$ and $\mathbf{12}_{\mathbf{dimer}}$, the related bicyclic with no πCC, reveals that the added 10 πe^- delocalization leads to a 3.1 kcal/mol stabilization. Published crystal structures of derivatives of $\mathbf{9}_{\mathbf{dimer}}$ and $\mathbf{12}_{\mathbf{dimer}}$ also show shorter N···N distances in the former than the latter, in agreement with the calculated dimerization energies (see Figure 8).[60,61,63,65] In $\mathbf{10}_{\mathbf{dimer}}$, an even higher dimerization energy is expected, since no imidazole sextet is disrupted as the imidazolium sextet is enhanced. This difference, however, is quite small. On the other hand, dimerization of **11** should disrupt the imidazole sextet, weakening the H-bonding; this effect is observed as a 2.8 kcal/mol decrease in dimerization energy compared to $\mathbf{12}_{\mathbf{dimer}}$. In this case, the $\Delta\mathrm{NICS}(1)_{zz}$ = +2.4 ppm supports the idea that the diatropicity of the ring current is decreased upon dimerization. Such considerations for H-bonded system design would be of interest, since the H-bonding strength for the same guanidine moiety could be electronically tuned with a very slight change in sterics, i.e. the hydrogenation of double bonds. Though **9**, **11**, and **12** are known,[66,67] compound **10** is not likely to be thermodynamically stable in a chemical environment; its computed electronic energy, without thermal corrections, is 9.4 kcal/mol above that of its isomer **11**.

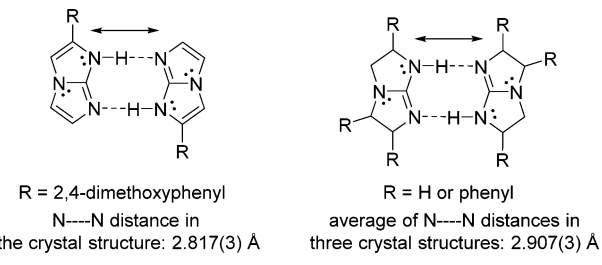

Figure 8. Comparison of X-ray crystal structure H-bond donor-acceptor distances for $\mathbf{9}_{\mathbf{dimer}}$ and $\mathbf{12}_{\mathbf{dimer}}$ derivatives.

CONCLUSIONS

The present survey has broadly explored the idea that H-bond strength can be modulated by resonance-mediated synergistic interactions with (anti)aromatic π-delocalization. The generality and robustness of this concept is solidly demonstrated by comparison of H-bonding energies of 24 five-membered heterocycles capable of πCC/H-bonding coupling vs reference structures that lack πCCs. Further confirmation is seen in these systems' magnetic behavior as revealed by H-bond-induced changes in $\mathrm{NICS}(1)_{zz}$ values. Recognition of this nonlocal interplay between (anti)aromaticity and H-bonding promises to improve understanding and effective modeling of H-bonding in nucleobase pairs and other heterocycles of biological and pharmaceutical importance. Generalization of the AMHB concept also offers guidance for the design and fine-tuning of selective interactions in organocatalysts and self-assembling materials.

ASSOCIATED CONTENT

Supporting Information

The Supporting Information is available free of charge on the ACS Publications website at DOI: 10.1021/jacs.5b12703.

Cartesian coordinates and total electronic energies for all systems considered, detailed procedure for placing $\mathrm{NICS}(1)_{zz}$ probe, and computational details for the enthalpies calculated in Figure 1 (PDF)

AUTHOR INFORMATION

Corresponding Authors

*jackson@chemistry.msu.edu
*jiwu@central.uh.edu

Notes

The authors declare no competing financial interest.

ACKNOWLEDGMENTS

This manuscript is dedicated to the memory of Professor Paul Schleyer. T.K. and J.E.J. gratefully acknowledge enabling computer assistance by Paul Reed. Research at Michigan State University (MSU) was supported by the National Science Foundation under award CHE-1362812, and for computing resources, the High Performance Computing Center at MSU.

REFERENCES

(1) Gilli, G.; Gilli, P. *J. Mol. Struct.* **2000**, *552*, 1−15.
(2) Fonseca Guerra, C.; Zijlstra, H.; Paragi, G.; Bickelhaupt, F. M. *Chem. - Eur. J.* **2011**, *17*, 12612−12622.
(3) Alder, R. W.; Bowman, P. S.; Steele, W. R. S.; Winterman, D. R. *Chem. Commun.* **1968**, *13*, 723−724.
(4) Inuzuka, K.; Fujimoto, A. *Bull. Chem. Soc. Jpn.* **1982**, *55*, 2537−2540.
(5) Inuzuka, K.; Fujimoto, A. *Spectrochim. Acta, Part A* **1984**, *40*, 623−627.
(6) Wu, J. I.; Jackson, J. E.; Schleyer, P. v. R. *J. Am. Chem. Soc.* **2014**, *136*, 13526−13529.
(7) Anand, M.; Fernández, I.; Schaefer, H. F.; Wu, J. I. *J. Comput. Chem.* **2016**, *37*, 59−63.
(8) Dewar, M. J. S. *Nature* **1945**, *155*, 50−51.
(9) Dewar, M. J. S. *Nature* **1950**, *166*, 790−791.
(10) Maksić, Z. B.; KovaČević, B. *J. Phys. Chem. A* **1999**, *103*, 6678−6684.
(11) Maksić, Z. B.; Glasovac, Z.; Despotović, I. *J. Phys. Org. Chem.* **2002**, *15*, 499−508.

DOI: 10.1021/jacs.5b12703
J. Am. Chem. Soc. 2016, 138, 3427−3432

(12) Despotović, I.; Maksić, Z. B.; Vianello, R. *New J. Chem.* **2007**, *31*, 52−62.
(13) Ian Storer, R.; Aciro, C.; Jones, L. H. *Chem. Soc. Rev.* **2011**, *40*, 2330−2346.
(14) Quiñonero, D.; Prohens, R.; Garau, C.; Frontera, A.; Ballester, P.; Costa, A.; Deyà, P. M. *Chem. Phys. Lett.* **2002**, *351*, 115−120.
(15) Saez Talens, V.; Englebienne, P.; Trinh, T. T.; Noteborn, W. E. M.; Voets, I. K.; Kieltyka, R. E. *Angew. Chem., Int. Ed.* **2015**, *54*, 10502−10506.
(16) Lu, T.; Wheeler, S. E. *Chem. - Eur. J.* **2013**, *19*, 15141−15147.
(17) Morris, P. A.; MacKenzie, D. H.; Masheter, H. C. *Br. J. Psychiatry* **1970**, *117*, 683−684.
(18) Zempleni, J.; Kuroishi, T. *Adv. Nutr.* **2012**, *3*, 213−214.
(19) Gaitonde, C. D.; Pathak, P. V. *J. Chromatogr., Biomed. Appl.* **1990**, *528*, 407−414.
(20) Spierings, E. H.; Rapoport, A.; Dodick, D.; Charlesworth, B. *CNS Drugs* **2004**, *18*, 1133−1141.
(21) Gao, Y.; Li, X.; Guo, J.; Sun, X.; Sun, Z. *Chemosphere* **2015**, *120*, 1−7.
(22) Kampik, A.; Arias-Puente, A.; O'Brart, D. P. S.; Vuori, M.-L.; Group, T. E. L. S. *J. Glaucoma* **2002**, *11*, 90−96.
(23) Dugger, J. A. *J. New Drugs* **1961**, *1*, 223−229.
(24) Kostyuk, P. G.; Molokanova, E. A.; Pronchuk, N. F.; Savchenko, A. N.; Verkhratsky, A. N. *Neuroscience* **1992**, *51*, 755−758.
(25) Frisch, M. J.; Trucks, G. W.; Schlegel, H. B.; Scuseria, G. E.; Robb, M. A.; Cheeseman, J. R.; Scalmani, G.; Barone, V.; Mennucci, B.; Petersson, G. A.; Nakatsuji, H.; Caricato, M.; Li, X.; Hratchian, H. P.; Izmaylov, A. F.; Bloino, J.; Zheng, G.; Sonnenberg, J. L.; Hada, M.; Ehara, M.; Toyota, K.; Fukuda, R.; Hasegawa, J.; Ishida, M.; Nakajima, T.; Honda, Y.; Kitao, O.; Nakai, H.; Vreven, T.; Montgomery, J. A., Jr.; Peralta, J. E.; Ogliaro, F.; Bearpark, M.; Heyd, J. J.; Brothers, E.; Kudin, K. N.; Staroverov, V. N.; Keith, T.; Kobayashi, R.; Normand, J.; Raghavachari, K.; Rendell, A.; Burant, J. C.; Iyengar, S. S.; Tomasi, J.; Cossi, M.; Rega, N.; Millam, J. M.; Klene, M.; Knox, J. E.; Cross, J. B.; Bakken, V.; Adamo, C.; Jaramillo, J.; Gomperts, R.; Stratmann, R. E.; Yazyev, O.; Austin, A. J.; Cammi, R.; Pomelli, C.; Ochterski, J. W.; Martin, R. L.; Morokuma, K.; Zakrzewski, V. G.; Voth, G. A.; Salvador, P.; Dannenberg, J. J.; Dapprich, S.; Daniels, A. D.; Farkas, O.; Foresman, J. B.; Ortiz, J. V.; Cioslowski, J.; Fox, D. J. *Gaussian09*; Revision D.01; Gaussian, Inc.: Wallingford, CT, 2013.
(26) Adamo, C.; Barone, V. *J. Chem. Phys.* **1999**, *110*, 6158−6170.
(27) Krishnan, R.; Binkley, J. S.; Seeger, R.; Pople, J. A. *J. Chem. Phys.* **1980**, *72*, 650−654.
(28) Clark, T.; Chandrasekhar, J.; Spitznagel, G. W.; Schleyer, P. V. R. *J. Comput. Chem.* **1983**, *4*, 294−301.
(29) Gill, P. M. W.; Johnson, B. G.; Pople, J. A.; Frisch, M. J. *Chem. Phys. Lett.* **1992**, *197*, 499−505.
(30) Frisch, M. J.; Pople, J. A.; Binkley, J. S. *J. Chem. Phys.* **1984**, *80*, 3265−3269.
(31) Thanthiriwatte, K. S.; Hohenstein, E. G.; Burns, L. A.; Sherrill, C. D. *J. Chem. Theory Comput.* **2011**, *7*, 88−96.
(32) DiLabio, G. A.; Johnson, E. R.; Otero-de-la-Roza, A. *Phys. Chem. Chem. Phys.* **2013**, *15*, 12821−12828.
(33) Dunning, T. H. *J. Chem. Phys.* **1989**, *90*, 1007−1023.
(34) Kendall, R. A.; Dunning, T. H.; Harrison, R. J. *J. Chem. Phys.* **1992**, *96*, 6796−6806.
(35) Dunning, T. H.; Peterson, K. A.; Wilson, A. K. *J. Chem. Phys.* **2001**, *114*, 9244−9253.
(36) Barone, V.; Cossi, M. *J. Phys. Chem. A* **1998**, *102*, 1995−2001.
(37) Cossi, M.; Rega, N.; Scalmani, G.; Barone, V. *J. Comput. Chem.* **2003**, *24*, 669−681.
(38) Perdew, J. P.; Burke, K.; Wang, Y. *Phys. Rev. B: Condens. Matter Mater. Phys.* **1996**, *54*, 16533−16539.
(39) Schleyer, P. v. R.; Manoharan, M.; Wang, Z.-X.; Kiran, B.; Jiao, H.; Puchta, R.; van Eikema Hommes, N. J. R. *Org. Lett.* **2001**, *3*, 2465−2468.
(40) Thomas, I. R.; Bruno, I. J.; Cole, J. C.; Macrae, C. F.; Pidcock, E.; Wood, P. A. *J. Appl. Crystallogr.* **2010**, *43*, 362−366.
(41) Shahani, T.; Fun, H.-K.; Ragavan, R. V.; Vijayakumar, V.; Sarveswari, S. *Acta Crystallogr., Sect. E: Struct. Rep. Online* **2010**, *66*, o142−o143.
(42) Loh, W.-S.; Fun, H.-K.; Ragavan, R. V.; Vijayakumar, V.; Venkatesh, M. *Acta Crystallogr., Sect. E: Struct. Rep. Online* **2011**, *67*, o403−o404.
(43) De Camp, W. H.; Stewart, J. M. *Acta Crystallogr., Sect. B: Struct. Crystallogr. Cryst. Chem.* **1971**, *27*, 1227−1232.
(44) Loh, W.-S.; Fun, H.-K.; Ragavan, R. V.; Vijayakumar, V.; Sarveswari, S. *Acta Crystallogr., Sect. E: Struct. Rep. Online* **2011**, *67*, o151−o152.
(45) Shahani, T.; Fun, H.-K.; Ragavan, R. V.; Vijayakumar, V.; Sarveswari, S. *Acta Crystallogr., Sect. E: Struct. Rep. Online* **2010**, *66*, o1357−o1358.
(46) Sbit, M.; Dupont, L.; Dideberg, O.; Snoek, J. P.; Delarge, J. *Acta Crystallogr., Sect. C: Cryst. Struct. Commun.* **1987**, *43*, 718−720.
(47) Shi, H.; Zhu, H.-J.; Yin, P.-W.; Wang, J.-T.; Shi, X.-L. *Acta Crystallogr., Sect. E: Struct. Rep. Online* **2005**, *61*, o2246−o2247.
(48) Dai, B.-J.; Liu, Y.-Y.; Xu, Q.-B.; Hu, J.; Zhu, H.-J. *Acta Crystallogr., Sect. E: Struct. Rep. Online* **2009**, *65*, o675−o675.
(49) Jia, H.-S.; Li, Y.-F.; Liu, Y.-Y.; Liu, S.; Zhu, H.-J. *Acta Crystallogr., Sect. E: Struct. Rep. Online* **2008**, *64*, o855−o855.
(50) Sun, Y.-F.; Jia, H.-S.; Liu, S.; Luo, Z.-H.; Zhu, H.-J. *Acta Crystallogr., Sect. E: Struct. Rep. Online* **2007**, *63*, o3657−o3657.
(51) Kawai, H.; Kusuda, A.; Nakamura, S.; Shiro, M.; Shibata, N. *Angew. Chem., Int. Ed.* **2009**, *48*, 6324−6327.
(52) Shintani, R.; Soh, Y.-T.; Hayashi, T. *Org. Lett.* **2010**, *12*, 4106−4109.
(53) Liu, Y.-Y.; Wu, Z.-Y.; Shi, H.; Chu, Q.-Y.; Zhu, H.-J. *Acta Crystallogr., Sect. E: Struct. Rep. Online* **2008**, *64*, o2101−o2101.
(54) Shi, H.; Zhu, H.-J.; Wang, J.-T. *Acta Crystallogr., Sect. E: Struct. Rep. Online* **2006**, *62*, o233−o235.
(55) Yoshida, M.; Sassa, N.; Kato, T.; Fujinami, S.; Soeta, T.; Inomata, K.; Ukaji, Y. *Chem. - Eur. J.* **2014**, *20*, 2058−2064.
(56) Tamborini, L.; Pinto, A.; Smith, T. K.; Major, L. L.; Iannuzzi, M. C.; Cosconati, S.; Marinelli, L.; Novellino, E.; Lo Presti, L.; Wong, P. E.; Barrett, M. P.; De Micheli, C.; Conti, P. *ChemMedChem* **2012**, *7*, 1623−1634.
(57) Rybakov, V. B.; Babaev, E. V.; Belykh, E. N. *Acta Crystallogr., Sect. E: Struct. Rep. Online* **2002**, *58*, o126−o128.
(58) Guo, X.; Chen, W.; Chen, B.; Huang, W.; Qi, W.; Zhang, G.; Yu, Y. *Org. Lett.* **2015**, *17*, 1157−1159.
(59) Ermolat'ev, D. S.; Alifanov, V. L.; Rybakov, V. B.; Babaev, E. V.; Van Der Eycken, E. V. *Synthesis* **2008**, *2008*, 2083−2088.
(60) Lambert, P.; Evrard, G.; Durant, F. *Acta Crystallogr., Sect. B: Struct. Crystallogr. Cryst. Chem.* **1978**, *34*, 2654−2655.
(61) Cotton, F. A.; Murillo, C. A.; Wang, X.; Wilkinson, C. C. *Inorg. Chem.* **2006**, *45*, 5493−5500.
(62) Matosiuk, D.; Karczmarzyk, Z.; Krycki, A.; Fruzinski, A. *Anal. Sci.: X-Ray Struct. Anal. Online* **2005**, *21*, x19−x20.
(63) Isobe, T.; Fukuda, K.; Yamaguchi, K.; Seki, H.; Tokunaga, T.; Ishikawa, T. *J. Org. Chem.* **2000**, *65*, 7779−7785.
(64) Hauptmann, S. *Z. Chem.* **1973**, *13*, 200−200.
(65) Barraclough, P.; Black, J. W.; Cambridge, D.; Firmin, D.; Gerskowitch, V. P.; Glen, R. C.; Giles, H.; Gillam, J. M.; Hull, R. A. D.; Iyer, R.; Randall, P.; Shah, G. P.; Smith, S.; Whiting, M. V. *Private communication*, 1994, CSD entry identifier: LENREB.
(66) Shen, H.; Wang, Y.; Xie, Z. *Org. Lett.* **2011**, *13*, 4562−4565.
(67) Takeuchi, M.; Sakamoto, S.; Kawamuki, K.; Kurihara, H.; Nakahara, H.; Isomura, Y. *Chem. Pharm. Bull.* **1998**, *46*, 1703−1709.

DOI: 10.1021/jacs.5b12703
J. Am. Chem. Soc. 2016, 138, 3427−3432